2011

Multi-temporal unmixing analysis of Hyperion images over the Guanica Dry Forest

Maria C. Torres-Madronero
University of Puerto Rico

Miguel Velez-Reyes
University of Puerto Rico

Skip J. Van Bloem
University of Puerto Rico, skipvb@clemson.edu

Jesus D. Chinea
University of Puerto Rico

Recommended Citation

Torres-Madronero, Maria & Velez-Reyes, Miguel & Van Bloem, Skip J. & D. Chinea, Jesus. (2011). Multi-temporal unmixing analysis of Hyperion images over the Guanica Dry Forest. 1-4. 10.1109/WHISPERS.2011.6080870.

MULTI-TEMPORAL UNMIXING ANALYSIS OF HYPERION IMAGES OVER THE GUANICA DRY FOREST

Maria C. Torres-Madronero, Miguel Velez-Reyes, Skip J. Van Bloem, Jesus D. Chinea
Laboratory for Applied Remote Sensing and Image Processing, University of Puerto Rico-Mayaguez, PR

ABSTRACT

This paper presents a methodology to analyze time-series data from Hyperion to study seasonal vegetation dynamics on the Guánica Dry Forest in Puerto Rico. Unmixing analysis is performed over ten near-cloud-free Hyperion images collected in different months in 2008. Abundance maps and endmembers estimated from the unmixing procedure are used to analyze the seasonal changes in the forest. Results from the analysis are compared with published knowledge of the Guanica Forest phenology.

Index Terms— unmixing, multi-temporal image analysis, Hyperion, Guanica Dry Forest.

1. INTRODUCTION

The potential of high spectral resolution imaging technology to improve our knowledge of biodiversity patterns and processes remains largely untapped because of the lack of information extraction techniques that take full advantage of the information in the spatial, spectral, and temporal domains. Spectral information captured with hyperspectral remote sensor can be modeled as the linear combination of several non-homogeneous spectral signatures of the materials in the sensor field of view. The linear mixing model can be formulated as $\mathbf{y} = \mathbf{Sa} + \mathbf{w}$, where $\mathbf{y} \in \Re^n$ is the measured signature by the hyperspectral sensor, $\mathbf{S} \in \Re^{nxp}$ is a collection of p spectral signatures of constituent elements called endmembers, $\mathbf{a} \in \Re^p$ is the abundance vector, and $\mathbf{w} \in \Re^n$ represents the noise. For an image, the mixing model can be expressed in matrix form as $\mathbf{Y} = \mathbf{SA} + \mathbf{W}$, where $\mathbf{Y} \in \Re^{nxm}$ is the matrix of all spectral signatures in the image, m is the number of pixels, and $\mathbf{A} \in \Re^{pxm}$ is the matrix of abundance vectors. Solving the unmixing problem means to find the number of endmembers p, the endmember matrix **S,** and the fractional maps **A** for a given image **Y**.

The use of unmixing for multi-temporal analysis of remote sensing data has been researched in the past. For instance, Du et al. [1] described a change detection approach based in the linear mixing model for multi-temporal CASI images over crop fields. Change detection is done over the endmember matrix and abundance maps estimated for each image. A change is detected when the number of endmembers for each image changes or the difference between abundance maps is greater than a given threshold. Okin [2] proposed the relative spectral mixture analysis (RSMA) technique for multi-temporal analysis of MODIS multispectral imagery. RSMA defines each pixel in an image as the linear combination of green vegetation, nonphotosynthetic vegetation (i.e. branches, stem), litter cover, and snow cover endmembers. The RSMA estimates changes in abundance with respect to a reference time and assumes that endmember spectral signatures are time invariant.

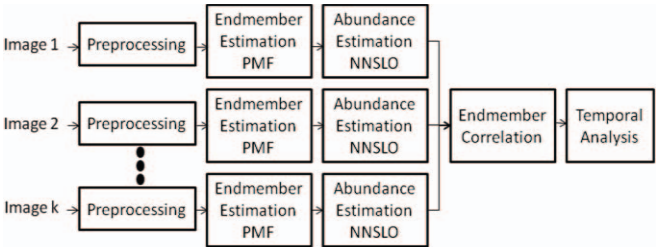

Fig. 1. Proposed Multi-temporal HSI Analysis Scheme.

We study an application of unmixing for multi-temporal analysis of Hyperion images captured over the Guanica Dry Forest. This paper describes the proposed framework for multi-temporal analysis, and unmixing results. Seasonal changes over the Guánica Dry Forest are identified using abundance maps estimated from Hyperion images.

2. MULTI-TEMPORAL HSI ANALYSIS

Using the high-spectral resolution provided by a hyperspectral sensor and the techniques for unmixing, we are developing a methodology to analyze multi-temporal imagery over a forest ecosystem. The methodology used in this research is summarized in Fig. 1. First, endmember extraction is done in each image using. Abundance maps are then estimated and the endmembers are correlated. Temporal analysis is done using the estimated endmembers as well as the abundance maps.

978-1-4577-2201-1/11/$26.00 ©2011 IEEE

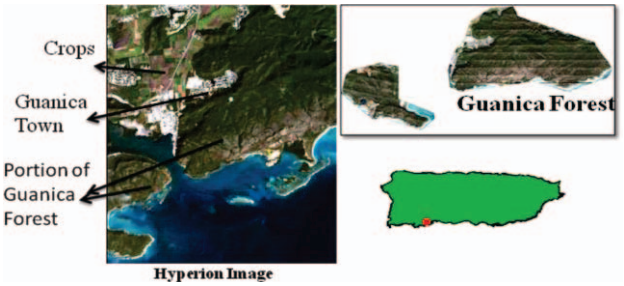

Fig. 2. True color composite of Hyperion image over Guanica Dry Forest.

2.1 Hyperion

The Hyperion sensor is part of the sensor suite in the EO-1 satellite launched in November 2000. Hyperion images consist of 240 spectral bands in the 400 nm to 2500 nm spectral range with a spatial resolution of 30 m. Hyperion has a swath of 7.7 km and captures a scene of 7.7 km by 185 km. The sensor can collect data on the nadir path (look angle from -5.975° to 5.975°), west path (look angle from 5.975° to 17.433°), and east path (look angle sensor from -17.433° to -5.975°). West path and east path images are collected seven and nine days after off-nadir view. Images collected from 2003 to the present are available in the US Geological Survey web page (http://eo1.usgs.gov). The USGS has available Hyperion imagery at Level 1R and Level 1GST. In this work, Level 1R data that consists of images already with radiometric corrections are used.

2.2 Preprocessing

Hyperion data have several stripes in different bands. A median filter was used to eliminate these corrupted pixels [3]. The FLAASH Atmospheric Correction Code available in ENVI was used for atmospheric correction. Uncalibrated bands and noise bands were eliminated. Bands 1 to 13, 58 to 81, 98 to 100, 119 to 134, 164 to 196, and 217 to 240 were eliminated, and an image cube of 127 bands was obtained. A water mask was applied to the image.

2.3 Endmember Estimation

Algorithms based on the Positive Matrix Factorization (PMF) have been proposed to solve the unmixing problem [4, 5]. PMF based algorithms do not assume that there are pure pixels in the image, which is very important for low spatial resolution images such as Hyperion image. Given the number of endmembers *p*, the PMF is determined by solving the optimization problem:

$$\hat{\mathbf{S}}, \hat{\mathbf{A}} = \arg\min \left\| \mathbf{Y} - \mathbf{S}\mathbf{A} \right\|_2^2 \quad \text{subject to } s_{ij} > 0,\ a_{ij} > 0,\ \sum_i a_{ij} = 1 \tag{1}$$

The PMF extracts an endmember matrix $\hat{\mathbf{S}}$ and an abundance matrix $\hat{\mathbf{A}}$.

When the PMF is applied globally (i.e. over the entire image at once), the extracted endmembers did not agree well with the known vegetation types present in the image (e.g. upland forest vegetation, mangrove, and crops). Experimentally we found that local application to the different parts of the image resulted in endmembers that better agree with the known vegetation classes. Thus, a local approach was applied for endmember estimation. The full image was divided into six spatial subsets and each was processed with PMF. The estimated endmembers of each subset were related to the endmembers of others subsets using spectral angle distance. The average of similar endmembers was used to form a new endmember matrix $\bar{\mathbf{S}}$ for the full image and the abundances were determined using:

$$\hat{\mathbf{A}} = \arg\min \left\| \mathbf{Y} - \bar{\mathbf{S}}\mathbf{A} \right\|_2^2 \quad \text{subject to } a_{ij} > 0,\ \sum_i a_{ij} \le 1 \tag{2}$$

Once the endmembers and abundance maps were estimated for each image, the endmembers that represent the same class in the different images are identified. The identification is done using the abundance maps and the spectral signature shape.

3. MULTI-TEMPORAL ANALYSIS OF GUANICA FOREST

Guanica Forest is a tropical dry forest, designated as a UNESCO man and Biosphere Reserve in 1981 and a core site of the Atlantic Neotropical Domain of the US National Ecological Observatory Network (NEON). The 4,400ha forest is located in southwestern Puerto Rico (Fig 2). The

Month	Average	2008
Jan	27.686	21.59
Feb	21.844	9.398
Mar	33.274	73.406
Apr	53.594	45.72
May	78.994	37.338
Jun	53.594	109.982
Jul	53.848	17.018
Aug	91.186	114.3
Sep	125.476	413.258
Oct	129.794	84.328
Nov	91.694	37.084
Dec	40.132	12.7
Annual	801.116	976.122

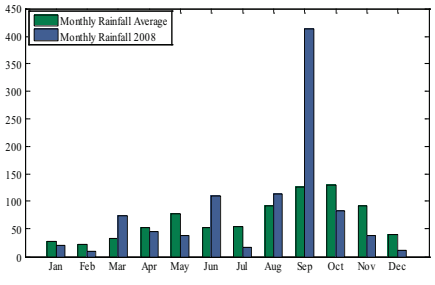

Fig. 3. Rainfall Record for the Guanica Dry Forest. Monthly Rainfall Average (in mm) in last 55 years and Monthly Rainfall in 2008 (in mm). Data obtained from:
* https://mi3.ncdc.noaa.gov//mi3qry/search.cfm

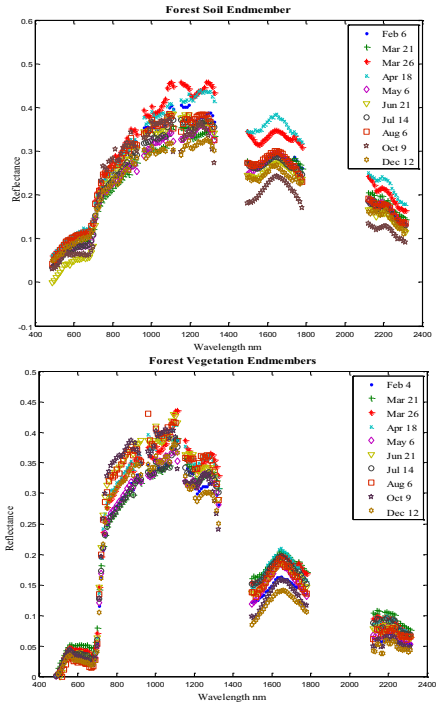

Fig. 4. Soil and vegetation endmembers estimated using PMF from the 2008 Hyperion images time series.

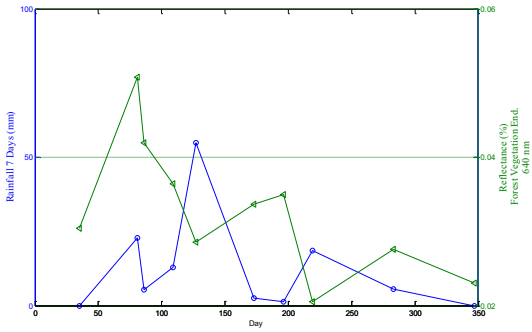

Fig.5. Temporal variation of the vegetation endmember at 640 nm. Comparison with rainfall report of 7 days before Image date.

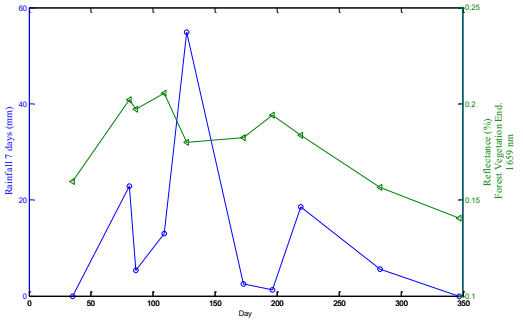

Fig. 6. Temporal variation of the vegetation endmember at 1650 nm. Comparison with rainfall report of 7 days previous to image date.

reserve includes several zones of grassland, cactus shrubland, upland forest, and mangrove forest. Rainfall averages 801 mm/year. Fig. 3 shows a summary of rainfall

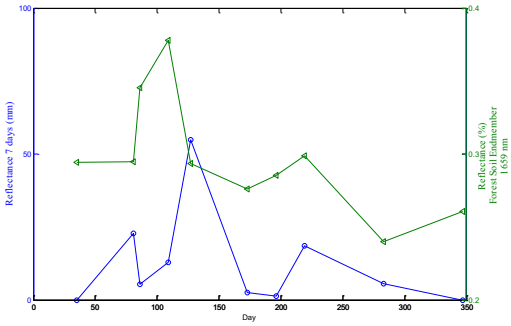

Fig.7. Temporal variation of the soil endmember in 1650 nm. Comparison with rainfall report of 7 days previous to image date.

records over the last 55 years. The Guánica Forest structure was studied between June 1975 and May 1976 by Lugo et al. [6] and between July 1981 and December 1983 by Murphy and Lugo [7]. Murphy and Lugo [7] observed that December to March were usually the driest months. Leaf area index decreased in the dry winter months, as well as, in a less proportion in summer months. Water deficit in the soil were presents in dry months. Soil recharges water usually from August to October. [6, 7].

About 63 images with minimal cloud cover were collected by Hyperion from 2004 to 2010 over a portion of Guanica Forest and these are available in the USGS website. The temporal analysis was done using the images collected in Feb. 4, March 21 and 26, April 18, May 6, June 21, July 14, Aug. 6, Oct. 9 and Dec. 12 of 2008. All images were collected on the nadir.

Six endmembers were estimated from each image: three vegetation endmembers (forest vegetation, mangrove, and crops), two soil endmembers (forest soil and crop soil), and one endmember for buildings. An additional endmember is estimated for images with clouds. The number of endmember is established from a prior knowledge of this area. Fig. 4 shows the forest soil and vegetation endmembers obtained for each image. Note, the consistency in the signature shape of the estimated endmembers. Fig 8 presents the abundance maps for these two endmembers.

3.2 Analysis of Results

There are three dominant factors that determine the vegetation spectral signature. The leaf reflectance from 350 nm to 700 nm is controlled by leaf pigments and chlorophyll. The near-infrared reflectance (700 nm to 1200 nm) is determined by the leaf cells. A healthy green leaf presents a reflectance between 40 to 60 percent. Finally, the vegetation spectral signature from 1300 nm to 2500 nm is determined by the interaction with water [8]. Fig. 5 shows the 640 nm band (a chlorophyll absorption band) of the forest vegetation endmember in different months. This band is appropriate to analyze annual chlorophyll dynamics.

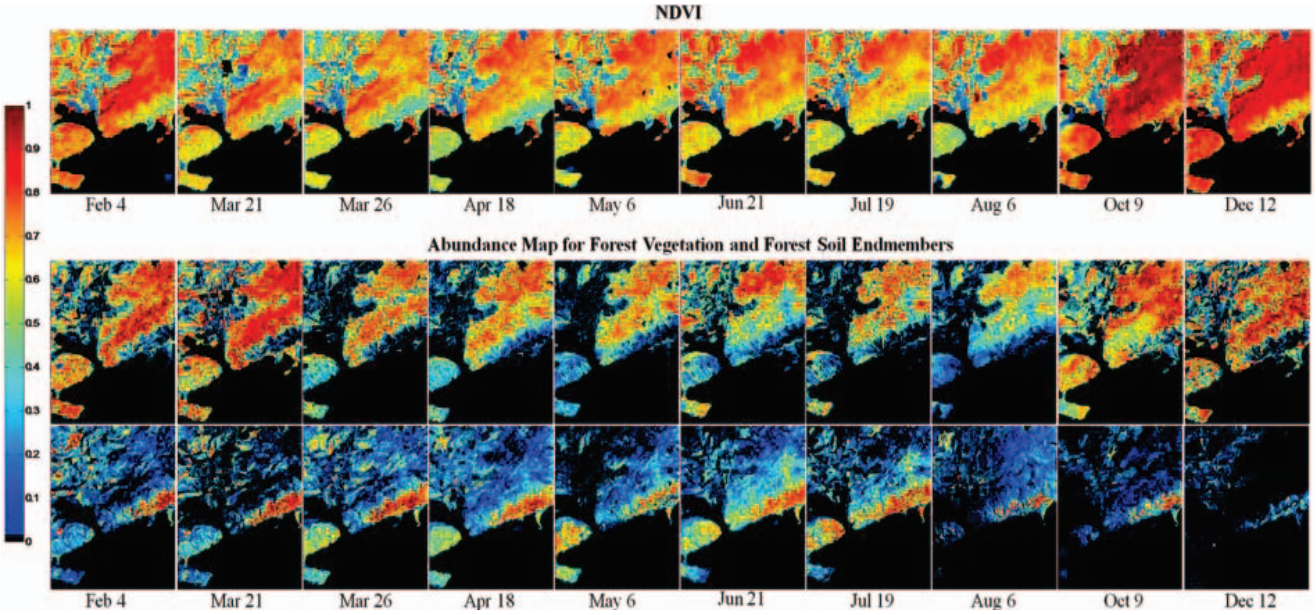

Fig. 8. NDVI and abundance maps for the vegetation and soil endmembers.

Lower reflectance in the 640 nm band is shown in the month of August (Fig. 5), corresponding a wet season.

Fig. 6 shows the 1650 nm band for the forest vegetation endmember in different months. Notice that the reflectance in the 1650 nm achieves the lowest percentage in December. The dry moths (i.e. winter and summer moths) have low soil moisture (Fig. 7).

Fig. 8 shows the abundance maps for forest vegetation and forest soil endmembers as well as the NDVI (Normalized Difference Vegetation Index) computed from the Hyperion image using bands in 854 nm and 640 nm. NDVI is widely used in temporal analysis and it is used for comparative purpose in this research. Fig. 8 shows the abundance maps for forest vegetation and forest soil endmembers as well as the NDVI (Normalized Difference Vegetation Index) computed from the Hyperion image using bands in 854 nm and 640 nm. NDVI is widely used in temporal analysis and it is used for comparative purpose in this research. Notice that vegetation abundance decreases from March to August, and from October to December it increases. Although, the NDVI presents a similar behavior, the changes in the abundance maps show more details in the forest dynamics. We can note that as the vegetation abundance decreases, the soil abundance increases from March to August.

4. CONCLUSIONS

The proposed framework for analysis of multi-temporal hyperspectral data based in unmixing analysis showed consistent results to understand seasonal changes in the Guanica Forest. Forest vegetation and forest soil endmembers abundance maps can be related to the rainfall events in the Guanica Forest. Future work will continue focusing on testing and validation of the approach.

5. ACKNOWLEDGMENTS

This work is supported by the NASA EPSCoR Program under Grant NNX09AV03A.

6. REFERENCES

[1] Q. Du, L. Wasson, R. King. “Unsupervised linear unmixing for change detection in multitemporal airborne hyperspectral imagery”. *MultiTemp 2005, International workshop on the*. pp. 136-140, (2005).

[2] G. S. Okin. “Relative spectral mixture analysis – A multitemporal index of total vegetation cover”. *J. in Remote Sens. Environ*. Vol 106 (4), pp. 467-479, (2006).

[3] D. Goodenough, A. Dyk, K. Olaf, J. Pearlman, H. Chen, T. Han, M, Murdoch, and C. West. “Processing Hyperion and ALI for forest classification”. *IEEE Trans. Geoscience and Remote Sensing*. Vol 41 (6), pp. 1321-1331, (2003).

[4] Y. Masalmah, and M. Vélez-Reyes, “A full algorithm to compute the constrained positive matrix factorization and its application in unsupervised unmixing of hyperspectral imagery.” *Proc. of SPIE,* Vol. 6966, (2008).

[5] S. Jia, and Y. Qian, “Constrained nonnegative matrix factorization for hyperspectral unmixing,” *IEEE Trans. Geoscience and Remote Sensing*, Vol 47 (1), pp. 161-173 (2009).

[6] A. Lugo, J. Gonzales, B. Cintron, and K. Dugger. “Structure, Productivity, and Transpiration of a Subtropical Dry Forest in Puerto Rico”. *Biotropica*. Vol 10(4), pp. 278-291, (1978).

[7] P. Murphy and A. Lugo. “Structure and Biomass of a Suptropical Dry Forest in Puerto Rico”. *Biotropica*. Vol 18(2), pp. 89-96, (1986).

[8] J. Jensen. *Remote Sensing of the Environment: An Earth Resource Perspective*. Pearson Prentice Hall. (2007).